



Synthesis, crystal structure, spectroscopic and photophysical studies of novel fluorinated quinazoline derivatives

Narva Deshwar Kushwaha^a, Sizwe J. Zamisa^b, Babita Kushwaha^a, Anamika Sharma^c, Francis Kayamba^a, Srinivas Reddy Merugu^a, Ab Majeed Ganai^a, Vincent A. Obakachi^a, Fernando Albericio^c, Rajshekhar Karpoomath^{a,*}

^a Department of Pharmaceutical Chemistry, Discipline of Pharmaceutical Sciences, College of Health Sciences, University of KwaZulu-Natal (Westville), Durban 4000, South Africa

^b School of Chemistry and Physics, University of KwaZulu-Natal, Private Bag X54001, Durban, 4000, South Africa

^c Peptide Science Laboratory, School of Chemistry and Physics, University of KwaZulu-Natal, Westville, Durban 4000, South Africa

ARTICLE INFO

Article history:

Received 31 August 2020

Revised 10 December 2020

Accepted 11 January 2021

Available online 19 January 2021

Keywords:

Quinazoline

Crystal structure

Photophysical properties

Density functional theory

ABSTRACT

A novel small library of seven fluorinated quinazoline derivatives was synthesized and for four of them, the crystal structures were solved by single X-ray diffractometer and compared the confirmation of molecules in solution-phase using 2D NOESY experiments. Taking advantage of the series prepared, we were able to describe the influence of various substituents on the core scaffold (fluorinated quinazoline) on its molecular conformations' intermolecular interactions and on the photoluminescent properties. The Hirshfeld surfaces were used to investigate the structure-directing effects of functional groups in controlling their solid-state behavior. Theoretical DFT calculations were carried out for getting additional knowledge on crystal-state interactions as compared to a gas phase. The photo-physical (UV and fluorescence) properties of all compounds have been studied. Among the series, five compounds exhibited excellent photoluminescent properties.

© 2021 Elsevier B.V. All rights reserved.

1. Introduction

In the past two decades there have been considerable efforts to develop new fluorophores with intramolecular charge transfer (ICT) emissions, as they have significant applications in non-linear optics (NLO) [1], organic-light emitting diodes (OLEDs), luminescence sensors [2], emissive material for sensor [3], dye-sensitized solar cells (DSSCs) [4] and field-effect transistors [5].

Quinazolines are important class of heterocyclic compounds which continue to attract appreciable attention in research because of their interesting photophysical (electronic absorption and emission) properties and extensive pharmacological applications. Quinazoline is a π -deficient, nitrogen containing fused benzopyrimidine aromatic ring system. This π -deficient aromatic ring is responsible for the intramolecular charge transfer (ICT) property [6–8]. The ICT property of quinazoline scaffold is essential luminescence characteristic and nonlinear optical (NLO) processes. The nitrogen atom of the quinazoline ring plays a critical role in the

formation of supramolecular assemblies [9] and sensors [10], by allowing protonation, hydrogen bond formation and chelation.

Further, quinazoline ring is present as a core moiety in a variety of bioactive natural products and some important marketed pharmaceutical drugs such as gefitinib [11], lapatinib [12], and erlotinib [13] (Fig. 1). From literature, it is quite evident that analogues of quinazoline also display a broad array of medicinal activities such as anticancer [14], antiviral [15], anti-tubercular [16], antimalarial [17], anticonvulsant [18], anti-inflammatory [19] and anti-hypertensive [20]. Owing to the comprehensive application of this pharmacophore, it continues to attract the attention of organic chemists to develop novel synthetic approaches to synthesize novel functionalized quinazolines and their derivatives [21,22].

Additionally, the presence of fluorine in organic molecules has considerable importance in both material science as well as pharmaceuticals [23]. Introducing fluorine into the molecules provides a unique way of achieving distinctive modification with minimal changes in structural configuration. Fluorinated organic compounds have potential application in organic light-emitting diodes (OLEDs) [24,25], organic photovoltaic devices (OPV) [26] and organic field-effect transistors (OTFT) [27]. In addition it is well documented that replacing a hydrogen atom of the natural substrate with fluorine may enhance biological activity [28] along with several other

* Corresponding author.

E-mail address: Karpoomath@ukzn.ac.za (R. Karpoomath).

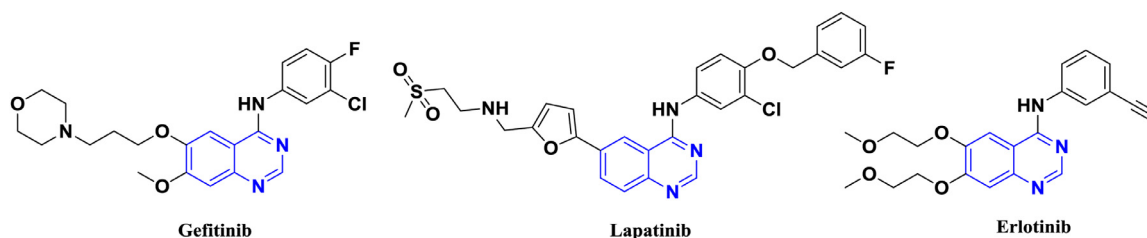


Fig. 1. Structures of some biologically active quinazoline.

biological properties such as solubility, lipophilicity, metabolic stability and binding selectivity [29]. Give this circumstance, we envisaged to synthesize novel fluorinated quinazoline derivatives and study the influence of the various substituents on the molecular conformation in gaseous, liquid and solid states and intermolecular interactions on the photoluminescent properties.

2. Experimental section

2.1. General consideration

All the fine chemicals, reagents and solvents were purchased from Sigma Aldrich and Merck and were used without further purification unless otherwise stated. The progress of the reactions and the purity of the compounds were monitored by thin-layer chromatography (TLC) on pre-coated silica gel plates procured from E. Merck and Co. (Darmstadt, Germany) visualized by UV lamp (254 or 365 nm). Purification was performed by using combi-flash (CombiFlash® NextGen 300+) column chromatography. The melting points of the synthesized compounds have been determined and uncorrected using a digital Stuart SMP10 melting point Apparatus. The Fourier transform infrared (FTIR) spectra were recorded in the spectral range of 400–4000 cm^{-1} on a Bruker Alpha FT-IR spectrometer using the ATR technique. The NMR spectra (^1H , ^{13}C , ^{19}F , & 2D) were recorded using CDCl_3 and $\text{DMSO}-d_6$ on Bruker AVANCE III 400 and 600 MHz spectrometer. Chemical shifts were determined relative to internal standard TMS at δ 0.0 parts per million (ppm) and the coupling constants were reported in Hertz. The multiplicities of the NMR resonances were abbreviated as s (singlet), d (doublet), dd (doublet of doublet), t (triplet), q (quartet), m (multiplet) and brs (broad singlet). X-ray crystallography analysis was performed on Bruker SMART APEX II, X-ray diffractometer.

2.2. Synthesis and characterizations

2.2.1. Synthesis and spectral characterization of intermediate compounds (2, 4, 5 and 6)

2.2.1.1. Synthesis of 2-amino-5-nitrobenzamide (2). To the solution of 2-amino-5-nitrobenzoic acid (30 g, 164.83 mmol) and HOBT (26.70 g, 197.80 mmol) in DMF (150 mL) was added EDC.HCl (37.78 g, 197.80 mmol). The mixture was stirred at ambient temperature for 2 h then cooled to 0 $^\circ\text{C}$, added 28% ammonia solution and again stirred for 2 h at room temperature, the reaction mixture was monitored by TLC, after consumption of starting material poured into ice cold water precipitate was formed, filtered and dried under vacuum, washed with pentane, diethyl ether to afford yellow solid product (24.9 g, 83%); mp: 128–134 $^\circ\text{C}$; FTIR (ATR, V_{max} , cm^{-1}): 3412.37 (N–H str. of NH_2), 3300.44 (N–H str.), 3198 (Ar–H str.), 1667.46 (C=O str.), 1613.56 (Ar C=C str.), 1314.55 (Ar- NO_2 str.); ^1H NMR (600 MHz, $\text{DMSO}-d_6$, 25 $^\circ\text{C}$) δ 8.54 (s, 1H), 8.18 (brs, 1H), 8.00 (d, J = 8.99 Hz, 1H), 7.86 (brs, 2H), 7.36 (brs, 1H), 6.79 (d, J = 9.17 Hz, 1H). ^{13}C NMR (150 MHz, $\text{DMSO}-d_6$, 25 $^\circ\text{C}$) δ 169.6, 155.6, 134.8, 127.4, 126.3, 115.9, 112.0.

2.2.1.2. Synthesis of 2-(3,4-difluorophenyl)-6-nitro-2,3-dihydroquinazolin-4(1H)-one (4). To the solution of 2-amino-5-nitrobenzamide (10 g, 55.20 mmol) and 3,4-difluorobenzaldehyde (6.12 mL, 55.20 mmol) in methanol (20 mL) was added catalytic amount of *p*-toluenesulfonic acid (1.05 g, 5.52 mmol). The resultant mixture was reflux for 16 h, precipitate was formed, filtered and washed with methanol to afford yellow solid product (13.2 g, 78%); mp: 294–296 $^\circ\text{C}$; UV/vis (CH_3CN): λ_{max} = 344 nm; FTIR (ATR, V_{max} , cm^{-1}): 3477.23 (N–H str.), 3357.74 (N–H str.), 2973.94 (Ar–H str.), 1682.62 (C=O str.), 1487 (Ar C=C str.), 1324.68 (Ar- NO_2 str.), 1057 (C–F str.); ^1H NMR (600 MHz, $\text{DMSO}-d_6$, 25 $^\circ\text{C}$) δ 8.79 (brs, 1H), 8.57 (brs, 1H), 8.42 (d, J = 3.33 Hz, 1H), 8.11 (dd, J = 8.97 Hz, J = 2.77 Hz, 1H), 7.56 – 7.46 (m, 2H), 7.33 – 7.30 (m, 3H), 6.85 (d, J = 9.08 Hz, 1H), 6.05 (s, 1H). ^{13}C NMR (150 MHz, $\text{DMSO}-d_6$, 25 $^\circ\text{C}$) δ 161.2, 151.8, 150.4 – 148.6 (dd, $J_{\text{C-F}}$ = 246.5 Hz, $J_{\text{C-F}}$ = 14.3 Hz, 1C), 150.1 – 148.4 (dd, $J_{\text{C-F}}$ = 245.6 Hz, $J_{\text{C-F}}$ = 12.5 Hz, 1C), 138.7, 137.4, 129.0, 124.1, 123.4 – 123.4 (dd, $J_{\text{C-F}}$ = 6.6 Hz, $J_{\text{C-F}}$ = 3.31 Hz, 1C), 117.7 – 117.6 (d, $J_{\text{C-F}}$ = 17.3 Hz, 1C), 115.9 – 115.8 (d, $J_{\text{C-F}}$ = 17.3 Hz, 1C), 114.4, 112.6, 65.1. ^{19}F NMR (376 MHz, $\text{DMSO}-d_6$, 25 $^\circ\text{C}$) δ –137.74 (d, $J_{\text{F-F}}$ = 22.21 Hz, 1F), –138.35 (d, $J_{\text{F-F}}$ = 22.21 Hz, 1F).

2.2.1.3. Synthesis of 2-(3,4-difluorophenyl)-1,3-dimethyl-6-nitro-2,3-dihydroquinazolin-4(1H)-one (5). To the solution of 2-(3,4-difluorophenyl)-6-nitro-2,3-dihydroquinazolin-4(1H)-one (4 g, 13.10 mmol) in DMF was added potassium carbonate (9.04 g, 65.52 mmol) followed by iodomethane (4.09 mL, 65.52 mmol) for 16 h then poured into ice cold water precipitate was formed, filtered to get crude solid product. The crude was dissolved into DMSO (10 mL) and added water (50 mL) precipitate was formed filtered and dried under vacuum to afford yellow solid product (4.0 g, 91%); mp 220–222 $^\circ\text{C}$; ^1H NMR (400 MHz, $\text{DMSO}-d_6$, 25 $^\circ\text{C}$) δ 8.52 (d, J = 1.69 Hz, 1H), 8.20 (dd, J = 8.90 Hz, J = 1.87 Hz, 1H), 7.48 – 7.37 (m, 2H), 7.13 (s, 1H), 6.82 (d, J = 9.34 Hz, 1H), 6.04 (s, 1H), 2.97 (s, 3H), 2.89 (s, 3H). ^{13}C NMR (100 MHz, $\text{DMSO}-d_6$, 25 $^\circ\text{C}$) δ 159.3, 151.2 – 148.6 (dd, $J_{\text{C-F}}$ = 246.5 Hz, $J_{\text{C-F}}$ = 10.6 Hz, 1C), 150.1, 137.6, 134.6, 129.3, 124.0, 122.8, 118.6 – 118.4 (d, $J_{\text{C-F}}$ = 17.4 Hz, 1C), 115.7 – 115.6 (d, $J_{\text{C-F}}$ = 17.9 Hz, 1C), 113.4, 112.2, 77.0, 35.4, 31.71.

2.2.1.4. Synthesis of 6-amino-2-(3,4-difluorophenyl)-1,3-dimethyl-2,3-dihydroquinazolin-4(1H)-one (6). 2-(3,4-difluorophenyl)-1,3-dimethyl-6-nitro-2,3-dihydroquinazolin-4(1H)-one (4.52 g, 13.56 mmol) was added into the mixture of dioxane (28 mL), ethanol (20 mL) and water (12 mL) followed by ammonium chloride (3.62 g, 67.80 mmol). To the resultant mixture iron powder (2.27 g, 40.68 mmol) was added with vigorous stirring and then heated at 100 $^\circ\text{C}$ for 5 h. The reaction mixture was cool to room temperature and filtered through celite and washed with 10% MeOH/DCM. The filtrate was concentrated under reduce pressure and diluted with water then extracted with 10% IPA/ CHCl_3 (3 \times 50 mL). Organic phase was dried over anhydrous Na_2SO_4 , filtered and concentrated under reduce pressure to afford brown

Table 1
Crystallographic data and structural refinement details of 7b, 7e, 7f, and 7 g.

	7b	7e	7f	7 g
Chemical formula	4(C ₂₀ H ₂₁ F ₂ N ₃ O ₂)·3(H ₂ O)	8(C ₂₆ H ₂₃ F ₂ N ₃ O ₃)·3(C ₂ H ₆ O)	C ₂₃ H ₂₁ F ₂ N ₃ O ₄ S	C ₂₂ H ₁₈ F ₃ N ₃ O ₃ S
M _r	1547.63	3845.98	473.49	461.45
Crystal system, space group	Monoclinic, P2 ₁ /c	Monoclinic, P2 ₁ /c	Monoclinic, P2 ₁ /n	Monoclinic, C2/c
Temp. (K)	100	103	100	100
a, b, c (Å)	9.4635 (2), 13.2122 (3), 14.9413 (3)	29.2357 (7), 16.0622 (4), 10.0866 (2)	7.8508 (1), 15.7287 (2), 18.4655 (3)	26.6621 (9), 15.6874 (5), 10.1580 (4)
β (°)	92.210 (1)	99.026 (1)	98.257 (1)	109.399 (2)
V (Å ³)	1866.78 (7)	4677.9 (2)	2256.54 (6)	4007.5 (2)
Z	1	1	4	8
μ (mm ⁻¹)	0.11	0.10	0.20	0.22
Crystal size (mm)	0.36 × 0.24 × 0.17	0.29 × 0.18 × 0.11	0.26 × 0.18 × 0.13	0.31 × 0.22 × 0.14
T _{min} , T _{max}	0.698, 0.746	0.677, 0.746	0.703, 0.746	0.620, 0.746
No. of measured, independent and observed [I > 2σ(I)] reflections	23526, 4632, 3901	37523, 8667, 7337	35588, 5717, 4723	31843, 4985, 4703
R _{int}	0.021	0.041	0.028	0.049
(sin θ/λ) _{max} (Å ⁻¹)	0.669	0.606	0.673	0.669
R[F ² > 2σ(F ²)], wR(F ²), S	0.047, 0.129, 1.05	0.065, 0.151, 1.18	0.036, 0.098, 1.03	0.137, 0.313, 1.16
No. of reflections	4632	8667	5717	4985
No. of parameters	324	749	351	342
No. of restraints	140	111	14	59
Δρ _{max} , Δρ _{min} (e Å ⁻³)	0.99, -0.60	0.88, -0.47	0.36, -0.44	1.27, -0.79

liquid, yield: (2.9 g, 70%). ¹H NMR (400 MHz, DMSO-*d*₆, 25 °C) δ 7.40 – 7.33 (m, 1H), 7.20 – 7.14 (m, 1H), 7.08 (d, *J* = 2.54 Hz, 1H), 6.98 – 6.95 (m, 1H), 6.67 (dd, *J* = 8.62 Hz, *J* = 2.67 Hz, 1H), 6.42 (d, *J* = 8.59 Hz, 1H), 5.63 (s, 1H), 4.75 (s, 2H), 2.91 (s, 3H), 2.70 (s, 3H). ¹³C NMR (100 MHz, DMSO-*d*₆, 25 °C) δ 151.0 – 148.5 (dd, *J*_{C-F} = 245.91 Hz, *J*_{C-F} = 12.76 Hz, 1C), 150.8 – 148.2 (dd, *J*_{C-F} = 247.61 Hz, *J*_{C-F} = 12.76 Hz, 1C), 142.0, 137.6, 135.5, 133.5, 120.6, 118.7, 118.2 – 118.0 (d, *J*_{C-F} = 17.89 Hz, 1C), 116.1 – 115.9 (d, *J*_{C-F} = 7.24 Hz, 1C), 115.6, 113.0, 78.0, 37.0, 32.7.

2.2.2. General procedure for synthesis and spectral characterization of derivatives (7a-c), (7d) and (7f-g)

2.2.2.1. General procedure A for synthesis of derivatives (7a-c).

To the suspension of 6-amino-2-(3,4-difluorophenyl)-1,3-dimethyl-2,3-dihydroquinazolin-4(1H)-one (6) (1.0 equiv) in DCM, were added triethyl amine (1.5 equiv), followed by appropriate acid chloride (1.5 equiv) at 0 °C. The resultant mixture was stirred at room temperature for 2 h, quenched with sodium bicarbonate solution and extracted with DCM (3 × 30 mL). The combined organic layer was dried over anhydrous Na₂SO₄, filtered and evaporated under reduce pressure to get crude product which were purified by combi-flash column chromatography using MeOH/DCM as an eluent to afford the respective title products.

2.2.2.2. General procedure B for synthesis of derivatives (7f-g).

To the solution of 6-amino-2-(3,4-difluorophenyl)-1,3-dimethyl-2,3-dihydroquinazolin-4(1H)-one (6) (1.0 equiv) in DCM were added pyridine (8.0 equiv), followed by appropriate sulfonyl chloride (1.5 equiv) at 0 °C. The resultant mixture was stirred at room temperature for 16 h, quenched with 2N-HCl solution and extracted with DCM (3 × 20 mL). The combined organic layer was dried over anhydrous Na₂SO₄ and evaporated under reduced pressure to yield the crude, which were purified with diethyl ether, filtered to yield the pure title products.

2.2.2.1.1. Ethyl 2-((2-(3,4-difluorophenyl)-1,3-dimethyl-4-oxo-1,2,3,4-tetrahydroquinazolin-6-yl)amino)-2-oxoacetate (7a).

Yellow solid, Yield: 72%, mp: 110–115 °C; UV/vis (CH₃CN): λ_{max} = 319 nm; FTIR (ATR, *V*_{max}, cm⁻¹): 3337.34 (N-H str.), 2898.96 (Ar-H str.), 1692.16 (C=O str.), 1663.24 (Amide C=O str.), 1099.09 (C-F str.); ¹H NMR (400 MHz, DMSO-*d*₆, 25 °C) δ 10.69 (s, 1H), 8.21 (d, *J* = 2.48 Hz, 1H), 7.73 (dd, *J* = 8.60 Hz, *J* = 2.61 Hz, 1H), 7.44 – 7.37 (m, 1H), 7.28 – 7.23 (m, 1H), 7.02 – 7.00 (m, 1H), 6.64 (d, *J* = 9.07 Hz, 1H), 5.82 (s, 1H), 4.29 (q, *J* = 7.08 Hz, 2H),

2.90 (s, 3H), 2.81 (s, 3H), 1.30 (t, *J* = 7.21 Hz, 3H), ¹³C NMR (100 MHz, DMSO-*d*₆, 25 °C) δ 161.0, 160.6, 155.0, 150.9 – 148.3 (dd, *J*_{C-F} = 246.0 Hz, *J*_{C-F} = 15.1 Hz, 1C), 150.5 – 147.9 (dd, *J*_{C-F} = 247.9 Hz, *J*_{C-F} = 13.2 Hz, 1C), 143.0, 134.7 – 134.6 (d, *J*_{C-F} = 5.22 Hz, 1C), 128.4, 126.6, 122.8, 119.9, 118.2 – 118.0 (d, *J*_{C-F} = 17.6 Hz, 1C), 115.6 – 115.4 (d, *J*_{C-F} = 17.1 Hz, 1C), 115.4, 112.5, 77.0, 62.2, 34.9, 31.9, 13.8. ¹⁹F NMR (376 MHz, DMSO-*d*₆, 25 °C) δ –137.34 (d, *J*_{F-F} = 22.27 Hz, 1F), –138.10 (d, *J*_{F-F} = 22.11 Hz, 1F). MS *m/z* 426.0 [M+Na]⁺.

2.2.2.1.2. N-(2-(3,4-Difluorophenyl)-1,3-dimethyl-4-oxo-1,2,3,4-tetrahydroquinazolin-6-yl)isobutyramide (7b).

Yellow solid, Yield: 69%, mp: 177–180 °C; UV/vis (CH₃CN): λ_{max} = 310 nm; FTIR (ATR, *V*_{max}, cm⁻¹): 3271.56 (N-H str.), 2964.64 (Ar-H str.), 1663.45 (C=O str.), 1631.36 (C=O str.), 1513.08 (Ar C=C str.), 1099.84 (C-F str.); ¹H NMR (400 MHz, DMSO-*d*₆, 25 °C) δ 9.70 (s, 1H), 8.01 (d, *J* = 2.44 Hz, 1H), 7.64 (dd, *J* = 8.74 Hz, *J* = 2.62 Hz, 1H), 7.44 – 7.37 (m, 1H), 7.26 – 7.21 (m, 1H), 7.01 – 6.98 (m, 1H), 6.58 (d, *J* = 8.91 Hz, 1H), 5.78 (s, 1H), 2.90 (s, 3H), 2.78 (s, 3H), 2.56 – 2.51 (m, 1H), 1.08 (d, *J* = 6.72 Hz, 6H). ¹³C NMR (100 MHz, DMSO-*d*₆, 25 °C) δ 161.3, 150.4 – 148.2 (dd, *J*_{C-F} = 245.7 Hz, *J*_{C-F} = 12.9 Hz, 1C), 150.4 – 147.9 (dd, *J*_{C-F} = 246.4 Hz, *J*_{C-F} = 13.6 Hz, 1C), 141.9, 134.7, 130.7, 125.4, 122.89 – 122.82 (d, *J*_{C-F} = 6.9 Hz, 1C), 118.7, 118.1 – 118.0 (d, *J*_{C-F} = 17.2 Hz, 1C), 115.8, 115.6 – 115.4 (d, *J*_{C-F} = 17.0 Hz, 1C), 112.6, 77.1, 35.0, 34.8, 32.0, 19.5. ¹⁹F NMR (376 MHz, DMSO-*d*₆, 25 °C) δ –137.45 (d, *J*_{F-F} = 22.54 Hz, 1F), –138.26 (d, *J*_{F-F} = 22.77 Hz, 1F). MS *m/z* 396.0 [M+Na]⁺.

2.2.2.1.3. N-(2-(3,4-Difluorophenyl)-1,3-dimethyl-4-oxo-1,2,3,4-tetrahydroquinazolin-6-yl)cyclohexanecarboxamide (7c).

Off white solid, Yield: 81%, mp: 240–244 °C; UV/vis (CH₃CN): λ_{max} = 302 nm; FTIR (ATR, *V*_{max}, cm⁻¹): 3309.15 (N-H str.), 2924.78 (Ar-H str.), 1666 (C=O str.), 1639.73 (C=O str.), 1499.5 (Ar C=C str.), 1109.27 (C-F str.); ¹H NMR (400 MHz, DMSO-*d*₆, 25 °C) δ 9.68 (s, 1H), 8.02 (d, *J* = 2.75 Hz, 1H), 7.61 (dd, *J* = 8.65 Hz, *J* = 2.64 Hz, 1H), 7.44 – 7.37 (m, 1H), 7.26 – 7.21 (m, 1H), 7.01 – 6.98 (m, 1H), 6.57 (d, *J* = 8.94 Hz, 1H), 5.77 (s, 1H), 2.89 (s, 3H), 2.77 (s, 3H), 2.30 – 2.22 (m, 1H), 1.78 – 1.72 (m, 4H), 1.65 – 1.62 (m, 1H), 1.44 – 1.36 (m, 2H), 1.30 – 1.26 (m, 3H). ¹³C NMR (100 MHz, DMSO-*d*₆, 25 °C) δ 173.8, 161.3, 150.8 – 148.2 (dd, *J*_{C-F} = 247.1 Hz, *J*_{C-F} = 13.0 Hz, 1C), 150.4 – 147.8 (dd, *J*_{C-F} = 246.7 Hz, *J*_{C-F} = 12.0 Hz, 1C), 141.8, 134.7, 130.8, 125.3, 122.8 – 122.7 (dd, *J*_{C-F} = 6.9 Hz, *J*_{C-F} = 3.4 Hz, 1C), 118.6, 118.1 – 117.9 (d, *J*_{C-F} = 17.3 Hz, 1C), 115.8, 115.6 – 115.4 (d, *J*_{C-F} = 17.2 Hz, 1C), 112.6, 77.1, 56.0, 44.7, 35.0, 31.9, 29.15, 22.2. ¹⁹F NMR (376 MHz,

DMSO- d_6 , 25 °C) δ -137.46 (d, J_{F-F} = 22.49 Hz, 1F), -138.27 (d, J_{F-F} = 22.21 Hz, 1F). MS m/z 436.0 [M+Na] $^+$.

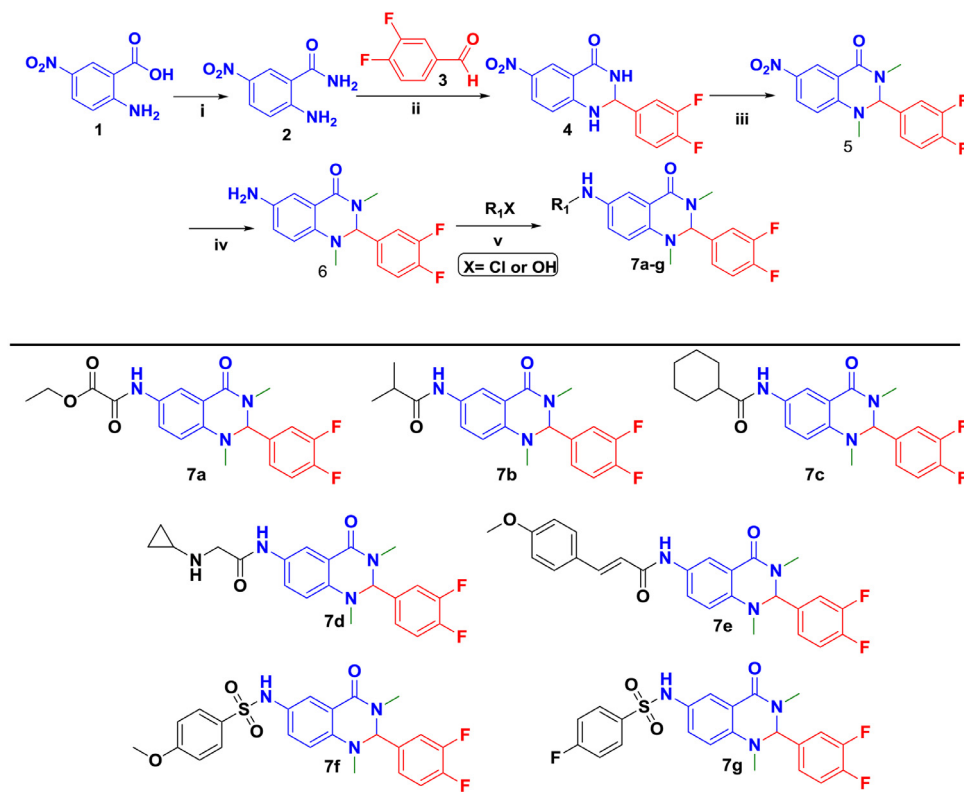
2.2.3. 2-(Cyclopropylamino)-N-(2-(3,4-difluorophenyl)-1,3-dimethyl-4-oxo-1,2,3,4-tetrahydroquinazolin-6-yl) acetamide (7d)

To the solution of 6-amino-2-(3,4-difluorophenyl)-1,3-dimethyl-2,3-dihydroquinazolin-4(1H)-one (6) (1.0 equiv) in DCM (10 mL) was added triethyl amine (1.5 equiv), followed by 2-bromoacetyl bromide (1.2 equiv) at 0 °C. The resultant mixture was stirred at room temperature for 2 h, precipitate was formed, filtered and washed with pentane to afford salt of 2-bromo-N-(2-(3,4-difluorophenyl)-1,3-dimethyl-4-oxo-1,2,3,4-tetrahydroquinazolin-6-yl)acetamide which were dissolved in DMF then added potassium carbonate (1.5 equiv), followed by cyclopropanamine (1.5 equiv) at room temperature. The resultant mixture was stirred at room temperature for 16 h, then diluted with ethyl acetate and washed with cold brine solution (3 \times 10 mL). The organic layer dried over anhydrous Na_2SO_4 , filtered and evaporated under reduce pressure to yield crude product which was recrystallized with ethanol to afford the pure yellow solid product: 71%, mp: 160–162 °C; UV/vis (CH_3CN): λ_{max} = 321 nm; FTIR (ATR, V_{max} , cm^{-1}): 3287.39 (N-H str.), 2969.97 (Ar-H str.), 1655.16 (C=O str.), 1636.82 (C=O str.), 1515.19 (Ar C=C str.), 1111.38 (C-F str.) ^1H NMR (400 MHz, DMSO- d_6 , 25 °C) δ 9.68 (s, 1H), 8.04 (d, J = 2.72 Hz, 1H), 7.63 (dd, J = 8.82 Hz, J = 2.59 Hz, 1H), 7.44 – 7.37 (m, 1H), 7.26 – 7.21 (m, 1H), 7.01 – 6.99 (m, 1H), 6.60 (d, J = 8.89 Hz, 1H), 5.78 (s, 1H), 3.29 (s, 2H), 2.90 (s, 3H), 2.78 (s, 3H), 2.18 – 2.13 (m, 1H), 0.39 – 0.34 (m, 2H), 0.31 – 0.26 (m, 2H). ^{13}C NMR (100 MHz, DMSO- d_6 , 25 °C) δ 169.9, 161.3, 150.8 – 148.2 (dd, J_{C-F} = 246.8 Hz, J_{C-F} = 12.1 Hz, 1C), 150.4 – 147.9

(dd, J_{C-F} = 248.0 Hz, J_{C-F} = 11.5 Hz, 1C), 142.1, 134.74 – 134.70 (d, J_{C-F} = 3.2 Hz, 1C), 130.0, 125.5, 122.85 – 122.82 (d, J_{C-F} = 3.2 Hz, 1C), 118.7, 118.1 – 118.0 (d, J_{C-F} = 18.2 Hz, 1C), 115.8, 115.6 – 115.4 (d, J_{C-F} = 17.5 Hz, 1C), 112.6, 77.1, 52.5, 35.0, 32.0, 30.1, 6.0. ^{19}F NMR (376 MHz, DMSO- d_6 , 25 °C) δ -137.43 (d, J_{F-F} = 22.40 Hz, 1F), -138.23 (d, J_{F-F} = 21.28 Hz, 1F). MS m/z 423.0 [M+Na] $^+$.

2.2.4. Synthesis of (E)-N-(2-(3,4-difluorophenyl)-1,3-dimethyl-4-oxo-1,2,3,4-tetrahydroquinazolin-6-yl)-3-(4-methoxyphenyl)acrylamide (7e)

To the solution of 6-amino-2-(3,4-difluorophenyl)-1,3-dimethyl-2,3-dihydroquinazolin-4(1H)-one (0.2 g, 0.65 mmol) in DMF (10 mL) were added DIPEA (0.229 mL, 1.31 mmol), EDC.HCl (0.188 g, 0.98 mmol) and HOBT (0.133 g, 0.98 mmol), stirred for 10 min. then (E)-3-(4-methoxyphenyl)acrylic acid (0.129 g, 0.72 mmol). The resultant mixture was stirred at room temperature for 16 h, poured into ice cold water precipitate formed was filtered to get crude solid, which was purified by column chromatography on silica gel (100–200 mesh) using MeOH/DCM as an eluent to afford the pure yellow solid, Yield: 85%, mp: 170–175 °C; UV/vis (CH_3CN): λ_{max} = 307 nm; FTIR (ATR, V_{max} , cm^{-1}): 3232.25 (N-H str.), 3231.03 (N-H str.), 1668.54 (C=O str.), 1636.89 (C=O str.), 1603.68 (Ar C=C str. alkene), 1510.78 (Ar C=C str.), 1111.09 (C-F str.); ^1H NMR (400 MHz, DMSO- d_6 , 25 °C) δ 10.04 (s, 1H), 8.11 (d, J = 2.84 Hz, 1H), 7.75 (dd, J = 8.79 Hz, J = 2.42 Hz, 1H), 7.56 (d, J = 8.33 Hz, 2H), 7.50 (d, J = 15.7 Hz, 1H), 7.45 – 7.38 (m, 1H), 7.28 – 7.23 (m, 1H), 7.03 – 6.99 (m, 3H), 6.67 (d, J = 15.26 Hz, 1H), 6.62 (s, 1H), 5.80 (s, 1H), 3.80 (s, 3H), 2.91 (s, 3H), 2.80 (s, 3H). ^{13}C NMR (100 MHz, DMSO- d_6 , 25 °C) δ 163.4, 161.3, 160.5, 150.8 – 148.3 (dd, J_{C-F} = 244.1 Hz, J_{C-F} = 9.5 Hz, 1C), 150.5 – 147.9 (dd, J_{C-F} = 247.5 Hz, J_{C-F} = 12.9 Hz, 1C), 142.0, 139.4, 134.7, 130.7, 129.2,



Scheme 1. Reagents and conditions: i) 28% aqueous ammonia solution, EDC.HCl, HOBT, DMF, 3–5 h; ii) pTSA, MeOH, 70 °C, 16 h; iii) CH_3I , K_2CO_3 , DMF, 0 °C - rt, 16 h; iv) Fe, NH_4Cl , Dioxane: EtOH: H_2O (7:5:3), 100 °C, 5 h; v) TEA, DCM, 0 °C - rt, 4 h. or Pyridine, DCM, 0 °C - rt, 16 h. or EDC.HCl, HOBT, DIPEA, DMF, rt, 16 h.

127.3, 125.3, 122.8, 119.7, 118.5, 118.2 – 118.0 (d, J_{C-F} = 17.4 Hz, 1C), 115.8, 115.6 – 115.4 (d, J_{C-F} = 17.3 Hz, 1C), 114.4, 112.7, 77.1, 55.2, 35.0, 32.0. ^{19}F NMR (376 MHz, DMSO- d_6 , 25 °C) δ -137.41 (d, J_{F-F} = 20.87 Hz, 1F), -138.20 (d, J_{F-F} = 22.37 Hz, 1F). MS m/z 486.0 $[\text{M}+\text{Na}]^+$.

2.2.2.2.1. *N*-(2-(3,4-Difluorophenyl)-1,3-dimethyl-4-oxo-1,2,3,4-tetrahydroquinazolin-6-yl)-4-methoxybenzenesulfonamide (7f):

Yellow solid, Yield: 81%, mp: 225–230 °C; UV/vis (CH₃CN): λ_{max} = 309 nm; FTIR (ATR, V_{max} , cm^{-1}): 3144.97 (N–H str.), 2998.25 (Ar–H str.), 1637.23 (C=O str.), 1507.04 (Ar C=C str.), 1251.94 (SO₂ asym.), 1154.55 (SO₂ sym.), 1021.06 (C–F str.); ^1H NMR (400 MHz, DMSO- d_6 , 25 °C) δ 9.72 (s, 1H), 7.57 (d, J = 9.48 Hz, 1H), 7.44 (d, J = 2.47 Hz, 1H), 7.41 – 7.36 (m, 1H), 7.16 – 7.07 (m, 2H), 7.02 (d, J = 8.66 Hz, 2H), 6.95 – 6.93 (m, 1H), 6.52 (d, J = 8.79 Hz, 1H), 5.76 (s, 1H), 3.78 (s, 3H), 2.85 (s, 3H). ^{13}C NMR (100 MHz, DMSO- d_6 , 25 °C) δ 162.3, 160.9, 150.9 – 148.3 (dd, J_{C-F} = 246.0 Hz, J_{C-F} = 12.55 Hz, 1C), 150.5 – 147.9 (dd, J_{C-F} = 246.2 Hz, J_{C-F} = 12.06 Hz, 1C), 143.3, 134.5, 130.9,

128.9, 128.3, 128.2, 122.8, 121.5, 118.1 – 117.9 (d, J_{C-F} = 16.6 Hz, 1C), 115.9, 115.4 – 115.2 (d, J_{C-F} = 18.4 Hz, 1C), 114.1, 113.0, 77.0, 55.5, 34.93, 31.9. ^{19}F NMR (376 MHz, DMSO- d_6 , 25 °C) δ -137.27 (d, J_{F-F} = 21.33 Hz, 1F), -138.03 (d, J_{F-F} = 22.03 Hz, 1F). MS m/z 472.0 $[\text{M}+\text{Cl}]^-$.

2.2.2.2.2. *N*-(2-(3,4-Difluorophenyl)-1,3-dimethyl-4-oxo-1,2,3,4-tetrahydroquinazolin-6-yl)-4-fluorobenzenesulfonamide (7g):

Yellow solid, Yield: 58%, mp: 180–185 °C; UV/vis (CH₃CN): λ_{max} = 354 nm; FTIR (ATR, V_{max} , cm^{-1}): 2987.92 (Ar–H str.), 1636.31 (C=O str.), 1514.22 (Ar C=C str.), 1317.80 (SO₂ asym.), 1148.41 (SO₂ sym.), 1092.03 (C–F str.); ^1H NMR (400 MHz, DMSO- d_6 , 25 °C) δ 9.89 (s, 1H), 7.71 – 7.67 (m, 2H), 7.44 – 7.34 (m, 4H), 7.15 – 7.08 (m, 2H), 6.96 – 6.93 (m, 1H), 6.54 (d, J = 8.81 Hz, 1H), 5.77 (s, 1H), 2.84 (s, 3H), 2.74 (s, 3H). ^{13}C NMR (100 MHz, DMSO- d_6 , 25 °C) δ 165.5 – 163.0 (d, J_{C-F} = 251.7 Hz, 1C), 160.7, 150.95 – 148.3 (dd, J_{C-F} = 246.7 Hz, J_{C-F} = 11.7 Hz, 1C), 150.5 – 147.9 (dd, J_{C-F} = 247.2 Hz, J_{C-F} = 12.6 Hz, 1C), 143.6, 135.5 – 135.4 (d, J_{C-F} = 2.4 Hz, 1C), 134.5, 129.8 – 129.7 (d, J_{C-F} = 10.3 Hz,

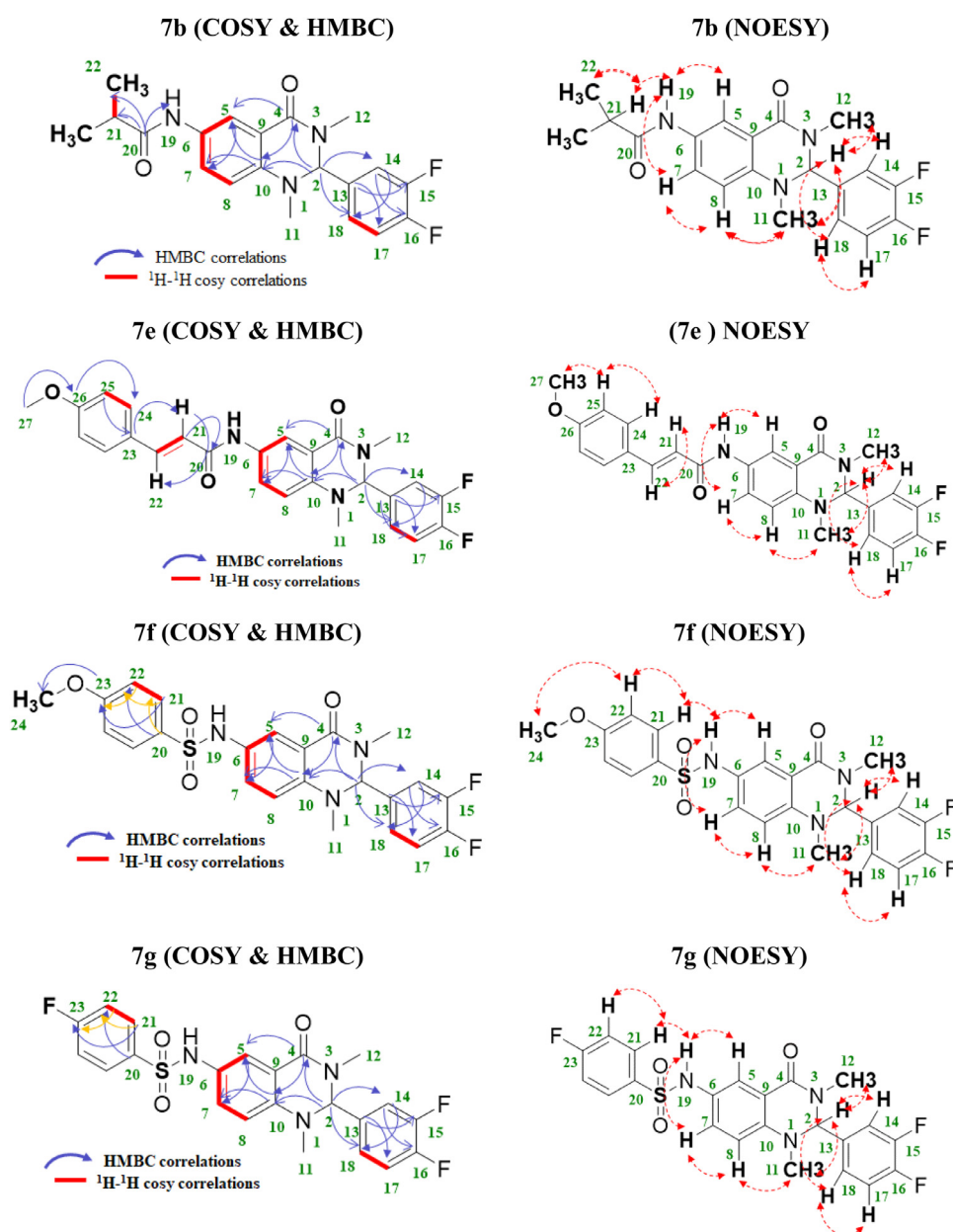


Fig. 2. 2D (NOESY, COSY, HSQC, and HMBC) correlations of compounds 7b, 7e, 7f and 7g.

1C), 128.8, 127.6, 122.9 – 122.8 (dd, $J_{C-F} = 6.3$ Hz, $J_{C-F} = 3.3$ Hz, 1C), 121.9, 118.1 – 118.0 (d, $J_{C-F} = 18.2$ Hz, 1C), 116.3 – 116.1 (d, $J_{C-F} = 23.0$ Hz, 1C), 115.8, 115.3 – 115.2 (d, $J_{C-F} = 16.9$ Hz, 1C), 113.1, 76.9, 34.8, 31.8. ^{19}F NMR (376 MHz, DMSO- d_6 , 25 °C) δ –106.25 (s, 1F), –137.25 (d, $J_{F-F} = 21.54$ Hz, 1F), –138.08 (d, $J_{F-F} = 20.17$ Hz, 1F). MS m/z 484.0 $[\text{M}+\text{Na}]^+$.

2.3. 2D NMR (NOESY, COSY, HSQC, and HMBC) analysis

The solution phase confirmation study was investigated using 2D NMR spectroscopic analysis on Bruker AVANCE III 400 MHz spectrometer. The 2D NMR investigations were performed in polar solvent (DMSO) by dissolving 20 mg of the compounds. The 2D NOESY (nuclear Overhauser effect spectroscopy) and COSY (correlation spectroscopy) experiment detect the proton-proton correlation through the space and bond respectively. The HSQC (Heteronuclear Single Quantum Coherence) experiment is used to determine proton-carbon single bond correlations while the HMBC (Heteronuclear Multiple Bond Correlation) experiment gives correlations between proton and carbons which are separated by two, three, and, sometimes in conjugated systems, four bonds.

2.4. Structure determination

Colourless, X-ray quality crystals were obtained by slow evaporation using DMSO for 7b and 7f whereas ethanol for 7e and 7 g. Crystal evaluation and data collection were done on

a Bruker Smart APEX2 diffractometer with a Mo $K\alpha$ radiation source ($\lambda = 0.71073$ Å) equipped with an Oxford Cryostream low-temperature apparatus. Initial cell matrix determination was done using 36 frames (0.5° phi-scan) from three series of scans at an exposure time of ten seconds per frame. Each of the three series of scans was collected at different starting angles and the APEXII [30] program suite used to index the reflections. The total number of images was based on results from the program COSMO [31] whereby the expected redundancy was to be 4.0% and completeness of 100% out to 0.75 Å. Cell parameters were retrieved using APEXII and refined using SAINT [32] on all observed reflections. Data reduction was performed using SAINT software, and the scaling and absorption corrections were applied using SADABS [33] multi-scan technique. The structures were solved by the direct method using the SHELXS [34] program and refined. The visual crystal structures were presented using, MERCURY [35,6] and Olex2 [36] system software. Non-hydrogen atoms were first refined isotropically and then by anisotropic refinement with full-matrix least squares based on F^2 using SHELXL [37]. All hydrogens were positioned geometrically, allowed to ride on their parent atoms, and refined isotropically. In all crystal structures, the 3,4-difluorophenyl moieties exhibited disorder over two positions which was resolved using PART instructions. The major component was found to have a site occupancy of 70.3% and 76% (7e), 58.1% (7b), 52.8% (7f) and 55% (7 g). Crystal data and structural refinement information are summarized in Table 1.

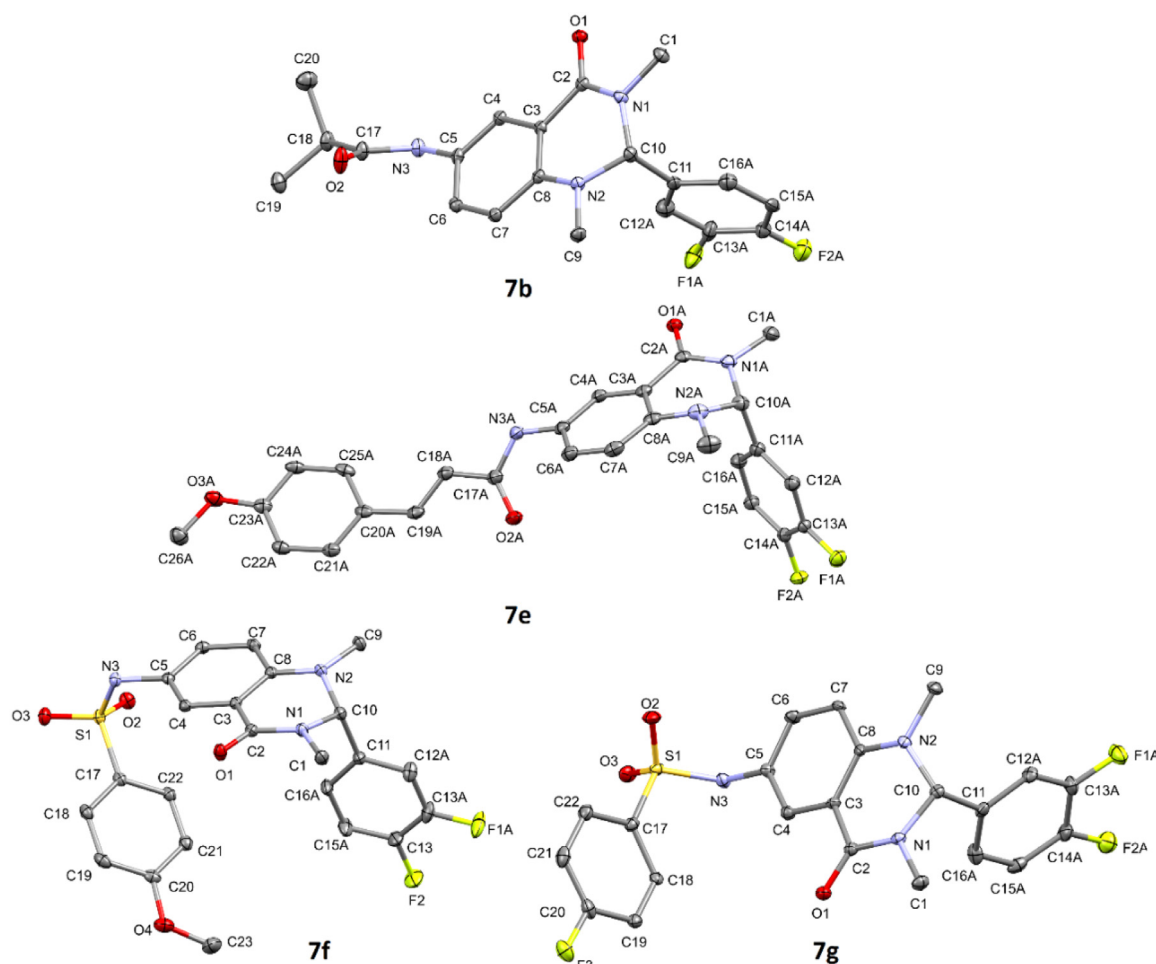


Fig. 3. ORTEP diagrams of compounds 7b, 7e, 7f, and 7 g drawn at 50% thermal ellipsoid probability. All hydrogen atoms, solvent molecules in 7b and 7e including one of the two quinazoline molecules of compound 7e have been omitted for clarity.

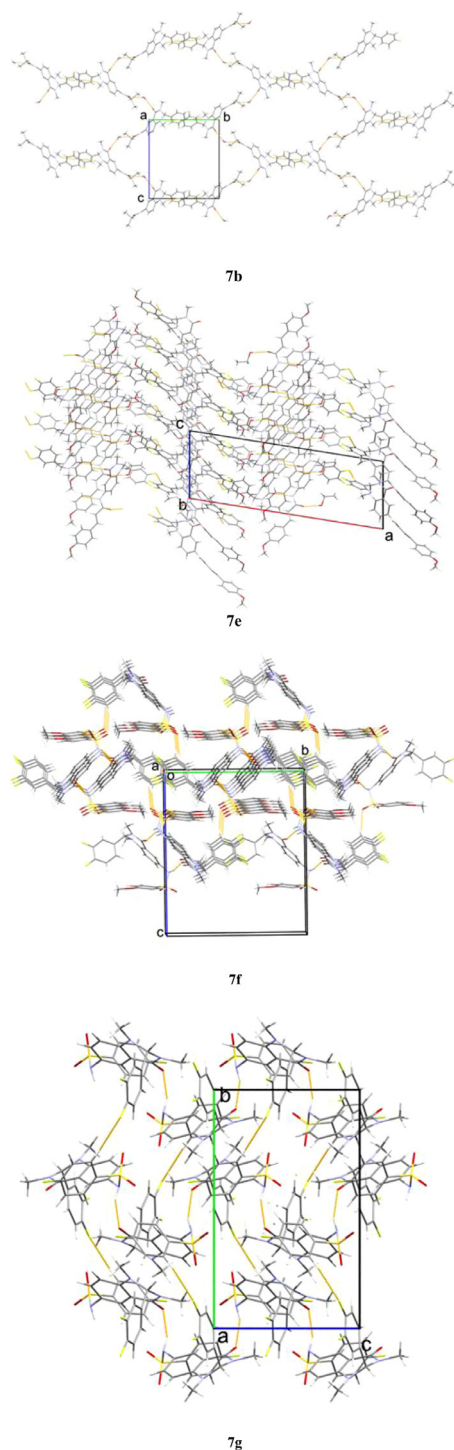


Fig. 4. Selected hydrogen bonding patterns (shown as dashed orange bonds) found in crystal packing of compounds 7b, 7e, 7f, and 7 g.

2.5. Hirshfeld surface analysis

Hirshfeld surface calculations were performed on compounds 7b, 7e, 7f and 7 g using *CrystalExplorer17* [38] whereby all Hirshfeld surfaces including 2D fingerprint [39–41] plots were generated using a high standard surface resolution. All bond lengths to hydrogen were automatically modified to typical standard neutron values ($C-H = 1.083 \text{ \AA}$, and $O-H = 0.983 \text{ \AA}$) when the crystallographic information file (CIF) of the respective compound was read into the *CrystalExplorer17* program [42]. The Hirshfeld surface

maps are that of normalized contact distance, d_{norm} , which is defined in terms of the distance to the nearest atoms outside (d_e), the distance to the nearest atoms inside (d_i) and the van der Waals radii of the two atoms external and internal to the surface [43]. The d_{norm} ranges used to map the Hirshfeld surfaces were -0.6316 to 1.4140 (7b), -0.6457 to 1.5251 (7e), -0.6022 to 1.5912 (7f) and -1.2575 to 1.5440 (7 g).

2.6. Theoretical calculation

A crystal unit was selected as the initial structure from the obtained crystals for theoretical calculations. DFT-B3LYP/6-311G++(d,p) methods in Gaussian09 were used to optimize the structures at default temperature of 298.15 K [44,45]. No solvent corrections were made with these calculations. Vibration analysis showed that the optimized structure indeed represents a minimum on the potential energy surface (no negative eigenvalues). TD-DFT calculations were performed using the same basis set as above to analyse the UV spectrum.

3. Result and discussion

3.1. Synthesis and spectral characterization

A brief description of synthetic route for all compounds is presented in [Scheme 1](#). 2-amino-5-nitrobenzamide (2) was synthesized adopting the procedure described by M. Tobe et al. [46], where the carboxylic acid was converted to the amide by treatment with aqueous ammonia in the presence of coupling reagent (EDC.HCl and HOBt) in DMF which was then treated with an aldehyde (3) in the presence of dehydrating agent (*p*TSA) in methanol to obtain cyclized product 2-(3,4-difluorophenyl)-6-nitro-2,3-dihydroquinazolin-4(1H)-one (4). The cyclized compound was alkylated with iodomethane in presence of K_2CO_3 in DMF at ambient temperature for 16 h followed by reduction with Fe/NH_4Cl in dioxane, ethanol and water (3:2:1) to yield 6-amino-2-(3,4-difluorophenyl)-1,3-dimethyl-2,3-dihydroquinazolin-4(1H)-one (6) which was treated with various acid, acid chlorides, and sulfonyl chlorides to yield a series of corresponding final compounds (7a-g). The structures of all the new compounds were confirmed by spectroscopic data obtained from UV, IR, NMR (1H , ^{13}C , ^{19}F and 2D). The IR spectra of all derivatives exhibited broad band in the regions of $1050-1150 \text{ cm}^{-1}$ are assigned for C-F stretching [47]. Furthermore, the 1H NMR spectrum of the compounds (7a-g) displayed distinct signals at around δ 10.69–9.68 assign for amide. The ^{13}C NMR spectrum of the compounds displayed some characteristic double doublet signals at around δ 150.9 – 150.4 and 150.5 – 150.4 ppm which showed J_{C-F} 247.1–244.1 Hz, 15.1– 9.5 Hz and 248.0 –246.4 Hz, 13.9 - 9.5 Hz respectively, verified the presence of two fluorine atoms in aromatic ring which was also confirmed by ^{19}F NMR spectrum.

3.2. 2D NMR (NOESY, COSY, HSQC, and HMBC) investigation of 7b, 7e, 7f and 7 g

The solution conformational investigation of compounds 7b, 7e, 7f and 7 g were carried out using 2D NMR (HMBC, HSQC, COSY and NOESY) analysis as depicted in [Fig. 2](#). Each molecule composed of 3,4 difluoro phenyl, 1,3-dimethyl-2,3-dihydroquinazolinone and amide (7b and 7e) or sulphonamide (7f and 7 g) moieties. The HMBC study of all molecules revealed that chiral carbon (2C) has a correlation with 4C, 10C, 14C and 18C through the bond and the NOESY study revealed that chiral proton (2H) showing connectivity with 11H, 12H, 14H and 18H through the space. It indicates that chiral proton is in the centre of 11H, 12H, 14H

and 18H. Furthermore, the 2D NMR study also revealed the absence of characteristic NOESY correlation between the proton of 1,3-dimethyl-2,3-dihydroquinazolinone and alkyl or aryl group of amide chain in compounds 7b, 7e and 7 g suggesting the non-existence of proximity (See ESI, Figure S21, S36 and S50). This indicates that the substituted amide groups of these compounds may away from 1,3-dimethyl-2,3-dihydroquinazolinone ring in the solution phase. For 7f the 2D NOESY (See ESI, Figure S43) failed to provide desired information about through space proton-proton connectivity between the aromatic proton of 1,3-dimethyl-2,3-dihydroquinazolinone ring and sulphonamide ring which is suggesting that the molecule is not in U shape in solution phase as confirmed by the crystal structure.

3.3. Crystal structure descriptions of 7b, 7e, 7f, and 7 g

The fluorinated quinazoline molecules of compounds 7b, 7e, 7f, and 7 g observed in their respective asymmetric units, are depicted in Fig. 3. Each molecule composes of a 3,4-difluorophenyl, 1,3-dimethyl-2,3-dihydroquinazolinonyl, amide (7b and 7e), sulfonamide (7f and 7 g) moieties. The 1,3-dimethyl-2,3-dihydroquinazolinone moiety in all the compounds was found to be non-planar with root mean squared deviation of 10 fitted atoms of the fused rings ranging from 0.110 Å to 0.123 Å. Furthermore, the 3,4-difluorophenyl groups were almost orthogonal with respect to the core 1,3-dimethyl-2,3-dihydroquinazolinonyl unit with dihedral angle between the two moieties ranging from 84.823° to 96.556°. Interestingly, it appears that the presence of the electron-donating substituent on the sulphonamide unit in 7f narrows C5–N3–S1–C17 torsion angle from –74.661 (7 g) to 56.3215 which results in 7f having a bent U-shaped molecular structure. All bond angles and distances are comparable to those of closely related structures [48,49].

Selected intermolecular hydrogen bonding parameters observed in 7b, 7e, 7f, and 7 g are listed in Table 2 while the hydrogen-bonding patterns are depicted in Fig. 4. Classical intermolecular N–H...O hydrogen bonds between the amide (7b and 7e) and sulphonamide (7f) link two neighbouring molecules to form a 14-membered ring with a graphset notation $R_2^2(14)$. Another N–H...O hydrogen-bonding pattern observed in 7e and 7 g sew together neighbouring molecules to form chains that propagate along the crystallographic c axis. Since 7b and 7e contained polar, protic solvent molecules, O–H...O hydrogen bonds were also observed

Table 2
Selected hydrogen-bonding parameters (Å, °) for 7b, 7e, 7f, and 7 g.

D–H...A	D–H	H...A	D...A	D–H...A
Compound 7b				
O3–H3A...O2 ⁱ	0.87	1.91	2.756 (2)	164
O3–H3B...O1	0.87	1.96	2.811 (2)	166
N3–H3...O1 ⁱⁱ	0.88	2.02	2.897 (2)	177
Compound 7e				
N3A–H3A...O1A ⁱ	0.88	1.98	2.854 (3)	173
N3B–H3B...O1B ⁱⁱ	0.88	2.01	2.855 (3)	160
C12C–H12C...F1A ⁱⁱⁱ	0.95	2.31	3.248 (8)	171
O4–H4...O2A	0.84	1.92	2.753 (3)	169
Compound 7f				
C19–H19...O2 ⁱ	0.95	2.35	3.2967 (2)	174
C15B–H15B...O3 ⁱⁱ	0.95	2.36	3.228 (5)	151
N3–H3...O1 ⁱⁱⁱ	0.88 (1)	1.96 (1)	2.817 (1)	166
Compound 7 g				
N3–H3...O1 ⁱ	0.88	1.95	2.739 (8)	149
C21–H21...F2B ⁱⁱ	0.95	2.23	3.05 (2)	144
C16B–H16B...F1B ⁱⁱⁱ	0.95	1.18	2.02 (2)	143

Symmetry codes: 7b (i) $x, -y - 1/2, z - 1/2$; (ii) $-x + 1, -y, -z$; 7e (i) $-x + 1, -y + 1, -z + 2$; (ii) $x, -y + 3/2, z - 1/2$; (iii) $-x, -y + 1, -z + 2$; 7f (i) $x - 1, y, z$; (ii) $-x + 3/2, y + 1/2, -z + 1/2$; (iii) $-x + 1, -y + 1, -z$; 7 g (i) $x, -y + 1, z + 1/2$; (ii) $x - 1/2, y - 1/2, z$; (iii) $x, -y + 1, z - 1/2$.

in their respective crystal packing. The methanol molecule in 7e forms a dimer via O–H...O hydrogen bonds with the carbonyl oxygen of the amide functional group. On the other hand, the water molecule in 7b links the 1,3-dimethyl-2,3-dihydroquinazolinonyl's and amide's carbonyl oxygen atoms of neighbouring molecules via O–H...O hydrogen bonds to form a 2-D supramolecular structure shown in Fig. 4. Non-classical C–H...F hydrogen bonding patterns also exist in 7e and 7 g between the aromatic hydrogens and 3,4-difluorophenyl moieties' fluorine atoms of neighbouring molecules. Linking molecules in this manner result in the formation of 2-D supramolecular architectures which extend along the crystallographic ac planes. Lastly, the C–H...O hydrogen bonds between the aromatic hydrogens (H19 and H15B) and O2 and O3 atoms of neighbouring sulphonamide moieties also form 2-D supramolecular structures which grow along the crystallographic ab planes.

3.4. Hirshfeld surface analysis

The molecular interactions of compounds 7b, 7e, 7f, and 7 g were studied by Hirshfeld surface analysis, which detailed the proximity of intermolecular interactions in their respective crystal packing. The Hirshfeld d_{norm} surface maps and the corresponding fingerprint plots for the H...H, H...O/O...H, C...H/H...C, and F...H/H...F interactions are depicted in Fig. 5 and 6, respectively. The red areas on the Hirshfeld surfaces around the 1,3-dimethyl-2,3-dihydroquinazolinonyl moiety highlight the reciprocal O...H/H...O contacts which are represented by a pair of broad spikes in the lower left (donor) area of the fingerprint plot and they are attributed to the N–H...O and C–H...O hydrogen bonds. Generally, the sulfonamides have larger O...H/H...O contribution to the d_{norm} surface than the amide derivatives due to a higher number of oxygen atoms. The H...H contacts were found to be the major contributor to the Hirshfeld surfaces with the amide derivatives having higher percentage values than the sulfonamides. Interestingly, it appears that the presence of the sterically demanding isopropyl group in 7b results in the highest H...H and H...F/F...H contributions in this series. As for the sulfonamides, the decrease in the H...H and H...F/F...H contributions from 34.1% (7f) to 27.3% (7 g) and from 16% (7f) to 14.5% (7 g) could be attributed to the widening of the C5–N3–S1–C17 torsion angle from 56.3(1) (7f) to –74.6(6) (7 g).

3.5. Photophysical studies

The UV-vis and fluorescence data for compounds 7a-g were acquired in acetonitrile at 25 °C and are summarized in Table 3. All compounds exhibit absorption maxima in the range 302–354 nm and 215–252 nm, which could be attributed to $n-\pi^*$ and $\pi-\pi^*$ electronic transitions, respectively. Replacing the oxalyl unit in 7a with a more conjugated (E)–1-methoxy-4-(ethenyl)benzene unit in 7e, causes a hypsochromic shift of the absorption maxima from 252 nm (7a) to 218 nm (7e) and 319 nm (7a) to 307 nm (7e). Furthermore, the presence of these conjugated moieties appears to

Table 3
Summarized details from UV and fluorescence spectra of compounds 7a-g.

Compound	$\lambda_{\text{max}}/\text{nm}$		Stokes shift/nm
	Absorption	Emission	
7a	252, 319	-	-
7b	220, 310	454	144
7c	220, 302	456	154
7d	225, 321	437	116
7e	218, 307	-	-
7f	252, 309	443	134
7 g	215, 354	402	98

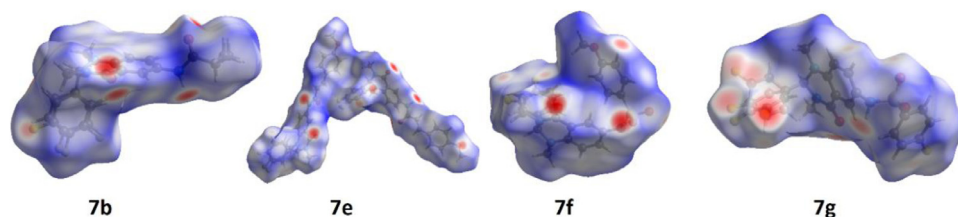
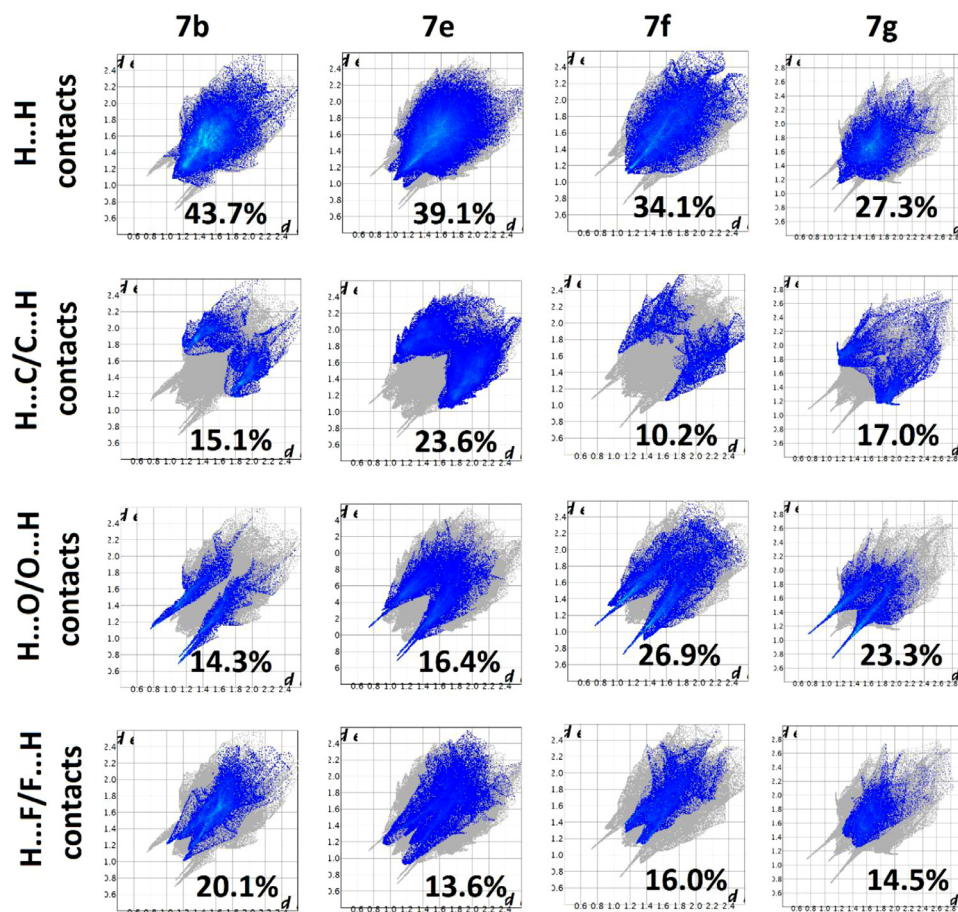
Fig. 5. d_{norm} mapped on Hirshfeld surfaces.

Fig. 6. 2D fingerprint plots depicting relative contributions of various intermolecular contacts.

quench the fluorescence ability of quinazoline. Similar to the 7e, the presence of aliphatic units in 7b-c also causes a hypsochromic shift of both absorption maxima relative to 7a. However, it appears that having an acyclic isopropyl unit (7b) causes a bathochromic shift from 310 nm to 302 nm, relative to 7c which has a cyclic hexyl unit. Interestingly, this activates the fluorescence ability of the quinazoline core and with emission maximum observed at 454 nm and 456 nm for 7b and 7c, respectively, and produce the two largest Stoke's shifts reported in this work. The presence of the *N*-alkylated cyclopropanyl in 7d not only causes significant bathochromic shifts of the absorption maxima, but also causes a hypsochromic shift of the emission maximum relative to that observed in 7b and 7c. Having an electron-donating group (-OMe) on the sulfonamide unit in 7f causes an absorption bathochromic shift from 354 nm (7 g) to 309 nm. Furthermore, whereas a large hypsochromic shift was observed from 354 nm (7 g) to 309 nm (7f).

3.6. Theoretical calculation

Gaussian09 program package [44] was employed for theoretical calculations. Geometry optimization of the structures was performed by using density functional theory (DFT) employing the B3LYP (Becke three parameters Lee–Yang–Parr exchange correlation functional), which combines the hybrid exchange functional of Becke with the gradient-correlation functional of Lee, Yang and Parr using 6-311G++(d,p) basis set was performed in the gas-phase at 298.15 K [45]. No solvent corrections were made with these calculations as gas-phase calculations frequently correspond quite well with crystal structures. Starting geometries for were taken from X-ray refined data. All the distorted geometry was removed while generating the input file. The optimized geometry results in the free molecule state were compared to those in the crystalline state. No negative vibrational modes were obtained. The DFT calculated structure and geometric parameters (bond lengths

Table 4
Total energy and frontier orbital energy [B3LYP/6-311++G(d,p)].

	7b	7e	7f	7 g
E_{total} (Hartree)	-1366.01639120	-1594.66296551	-1952.49439920	-1937.20477708
E_{HOMO}	-0.21182	-0.20315	-0.21891	-0.22316
E_{LUMO}	-0.06395	-0.06965	-0.06343	-0.06602
ΔE^a (eV)	4.33	3.63	4.23	4.27

^a $\Delta E = E_{\text{LUMO}} - E_{\text{HOMO}}$.

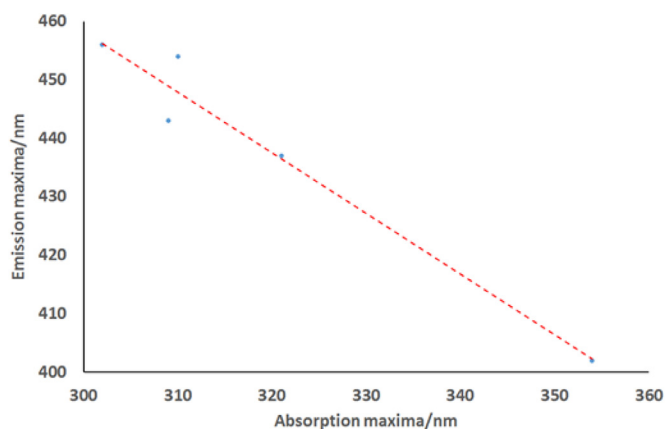


Fig. 7. Graph of absorption maxima v/s emission maxima. (Trendline: $y = -1.0374x + 769.55$ $R^2 = 0.9617$) Plotting a graph of absorption maxima against emission maxima, reveals an inversely proportional relationship between the two variables (Fig. 7). This provides a reasonable approximation and tunability of fluorescent properties of quinazolinyl derivative bearing non-conjugated amide moieties.

and bond angles) agreed with each other. All optimized structures had a C1 point group.

The bond length between C9-O3 and N8-H54 in case of 7f, was found to be 1.225 Å and 1.014 Å which is slightly higher than carbonyl (C=O) (usually 1.22 Å) and NH of sulphonamide, indicating presence of inter molecular H-bonding. Similar pattern of H-bonding was also determined in case of 7b, 7e and 7 g as shown by the increase of bond length compared to usual.

Frontier Orbital Energy and TD DFT calculations

Molecular Total Energy and Frontier Orbital energy levels were calculated using DFT (Table 4). Energy gap (ΔE) has been calculated for all 4 crystals as shown in the Table 3.

The energy gap between HOMO and LUMO was calculated by the B3LYP method using the 6-311G++(d,p) basis set. The compounds showed an energy gap (ΔE) for HOMO \rightarrow LUMO in a range from 3.63 to 4.33 eV (Table 4). HOMO and LUMO are essential factors that affect bioactivity, chemical reactivity and electron affinity and ionization potential [50]. Thus, a study of the frontier orbital energy can provide useful information about the biological and chemical reaction mechanism. TD-DFT calculations have also been performed to bring insight into the absorption spectra of the derivatives to calculate the excited states [51].

Electronic transition properties including λ_{max} were calculated for all 4 crystals using TD-DFT calculations using Gaussian09 and the values of λ_{max} (both in nm and eV) and oscillator strength have been calculated as shown in Table 5. From the calculated absorption spectrum, in case of 7b, three intense bands were observed corresponding to transitions from HOMO to LUMO (367.93 nm), HOMO to LUMO+1 (324.41 nm) and HOMO to LUMO+2 (300.08 nm). In case of 7 g the most prominent transition was observed from HOMO to LUMO+1 (311.03 nm) based on the oscillator strength whereas in case of 7e HOMO to LUMO was the most intense one at 380.20 nm. In the case of 7f, shows

Table 5
Calculation of absorption spectra using TD-DFT calculations.

Compound	Transitions from	Calculated λ_{max} (nm)	λ_{max} (eV)	F
7b	HOMO-LUMO	367.93	3.37	0.0453
	HOMO-LUMO+1	324.41	3.82	0.0402
	HOMO-LUMO+2	300.08	4.13	0.0507
7e	HOMO-LUMO	380.20	3.26	0.6693
	HOMO-LUMO+1	361.48	3.43	0.0495
7f	HOMO-LUMO+2	327.36	3.79	0.0033
	HOMO-LUMO	349.13	3.55	0.0409
7 g	HOMO-LUMO+1	313.46	3.96	0.0040
	HOMO-LUMO+2	305.50	4.06	0.0991
	HOMO-LUMO	344.95	3.59	0.0442
	HOMO-LUMO+1	311.03	3.99	0.1482
	HOMO-LUMO+2	303.23	4.09	0.0041

one intense band envelope based on the oscillator strength, at $\lambda_{\text{max}} = 305.50$ nm compared to the other two signals at 349.13 and 313.46 nm. This intense band refers to the transition from HOMO to LUMO+2.

4. Conclusion

To conclude, we established the synthesis and characterization of fluorinated quinazoline based derivatives by IR and NMR spectroscopy. Further, the crystal structures of the compounds 7b, 7e, 7f and 7 g were determined by X-ray diffraction, and the molecular interactions in the crystal structures packing were appraised by Hirshfeld surface analysis. The crystal structure analysis revealed that an electron-donating group on the sulphonamide core as presented in 7f constricted the C5-N3-S1-C17 torsion angle attaining a bent, U-shaped molecular structure. However, in solution phase, NOESY NMR experiment indicated no such U shape bent between the 1,3-dimethyl-2,3-dihydroquinazolinonyl ring and sulphonamide ring. Additionally, energy optimized structure obtained from the DFT calculations parameters revealed that the bond length between C9-O3 and N8-H54 in 7f, were slightly longer than carbonyl (C=O) and NH of sulphonamide, owing to intermolecular H-bonding. Notably, in compounds 7b, 7e and 7 g similar patterns were observed. Lastly, this class of compounds, i.e. compounds **7b-d** and **7f-g**, also exhibited promising photoluminescent properties.

Accession Codes

CCDC numbers 1956040, 1956041, 1956042 and 1956043 contain the supplementary crystallographic data for this paper. These data can be obtained free of charge via www.ccdc.cam.ac.uk/data_request/cif, or by emailing data_request@ccdc.cam.ac.uk.

Credit Author Statement

Narva Deshwar Kushwaha and Babita Kushwaha synthesized the compounds and drafted the manuscript. Sizwe J. Zamisa contributed to the crystal structures analysis by single X-ray diffract-

tometer and manuscript drafting. Anamika Sharma calculated the Theoretical DFT and contributed to the manuscript drafting. Francis Kayamba, Srinivas Reddy Merugu, Ab Majeed Ganai, Vincent A. Obakachi contributed to the data analysis and manuscript drafting. Rajshekhar Karpoomath and Fernando Albericio designed the experiments and supervised the project.

Declaration of Competing Interest

The authors declare that they have no known competing financial interests or personal relationships that could have appeared to influence the work reported in this paper.

Acknowledgment

The authors are thankful to the Discipline of Pharmaceutical Sciences, College of Health Sciences, University of KwaZulu-Natal (UKZN), Durban, South Africa, for providing all the necessary facilities. R.K. gratefully acknowledges National Research Foundation-South Africa (NRF-SA) for funding this project (grant nos. 103728, 112079 and 129247). The authors would also like to acknowledge fellow UKZN colleagues Dr. Vuyisa Mzozoyana (NMR spectroscopy).

Supplementary materials

Supplementary material associated with this article can be found, in the online version, at doi:10.1016/j.molstruc.2021.129951.

References

- [1] M. Pawlicki, H.A. Collins, R.G. Denning, H.L. Anderson, Two-photon absorption and the design of two-photon dyes, *Angew. Chem. Int. Ed.* 48 (2009) 3244–3266.
- [2] H. Meier, Conjugated oligomers with terminal donor–acceptor substitution, *Angew. Chem. Int. Ed.* 44 (2005) 2482–2506.
- [3] H.N. Kim, Z. Guo, W. Zhu, J. Yoon, H. Tian, Recent progress on polymer-based fluorescent and colorimetric chemosensors, *Chem. Soc. Rev.* 40 (2011) 79–93.
- [4] Y. Wu, W. Zhu, Organic sensitizers from D– π –A to D–A– π –A: effect of the internal electron-withdrawing units on molecular absorption, energy levels and photovoltaic performances, *Chem. Soc. Rev.* 42 (2013) 2039–2058.
- [5] H. Siringhaus, 25th anniversary article: organic field-effect transistors: the path beyond amorphous silicon, *Adv. Mater.* 26 (2014) 1319–1335.
- [6] E.V. Nosova, T.N. Moshkina, G.N. Lipunova, D.S. Kopchuk, P.A. Slepukhin, I.V. Baklanova, V.N. Charushin, Synthesis and photophysical studies of 2-(Thiophen-2-yl)-4-(morpholin-4-yl)quinazoline Derivatives, *Eur. J. Org. Chem.* 2016 (2016) 2876–2881.
- [7] S. Achelle, J.n. Rodríguez-López, F.o. Robin-le Guen, Synthesis and photophysical studies of a series of quinazoline chromophores, *J. Org. Chem.* 79 (2014) 7564–7571.
- [8] D. Liu, Z. Zhang, H. Zhang, Y. Wang, A novel approach towards white photoluminescence and electroluminescence by controlled protonation of a blue fluorophore, *Chem. Commun.* 49 (2013) 10001–10003.
- [9] A. Petitjean, L.A. Cuccia, J.M. Lehn, H. Nierengarten, M. Schmutz, Cation-promoted hierarchical formation of supramolecular assemblies of self-organized helical molecular components, *Angew. Chem. Int. Ed.* 41 (2002) 1195–1198.
- [10] C. Hadad, S. Achelle, I. Lopez-Solera, J.C. García-Martínez, J. Rodríguez-López, Metal cation complexation studies of 4-arylvinyl-2, 6-di (pyridin-2-yl) pyrimidines: effect on the optical properties, *Dyes Pigm.* 97 (2013) 230–237.
- [11] M.H. Cohen, G.A. Williams, R. Sridhara, G. Chen, R. Pazdur, FDA drug approval summary: gefitinib (ZD1839)(Iressa®) tablets, *Oncologist* 8 (2003) 303–306.
- [12] P. Wu, T.E. Nielsen, M.H. Clausen, FDA-approved small-molecule kinase inhibitors, *Trends Pharmacol. Sci.* 36 (2015) 422–439.
- [13] M.H. Cohen, J.R. Johnson, Y.-F. Chen, R. Sridhara, R. Pazdur, FDA drug approval summary: erlotinib (Tarceva®) tablets, *Oncologist* 10 (2005) 461–466.
- [14] I. Ahmad, An insight into the therapeutic potential of quinazoline derivatives as anticancer agents, *Med. Chem. Comm* 8 (2017) 871–885.
- [15] M. Schleiss, J. Eickhoff, S. Auerochs, M. Leis, S. Abele, S. Rechter, Y. Choi, J. Anderson, G. Scott, W. Rawlinson, Protein kinase inhibitors of the quinazoline class exert anti-cytomegaloviral activity in vitro and in vivo, *Antiviral Res.* 79 (2008) 49–61.
- [16] M.B. Harbut, B. Yang, R. Liu, T. Yano, C. Vilchère, B. Cheng, J. Lockner, H. Guo, C. Yu, S.G. Franzblau, Small molecules targeting mycobacterium tuberculosis type II NADH dehydrogenase exhibit antimycobacterial activity, *Angew. Chem.* 130 (2018) 3536–3540.
- [17] S. Madapa, Z. Tusi, A. Mishra, K. Srivastava, S. Pandey, R. Tripathi, S. Puri, S. Barta, Search for new pharmacophores for antimalarial activity. Part II: synthesis and antimalarial activity of new 6-ureido-4-anilinoquinazolines, *Bioorg. Med. Chem.* 17 (2009) 222–234.
- [18] V.G. Ugale, S.B. Bari, Quinazolines: new horizons in anticonvulsant therapy, *Eur. J. Med. Chem.* 80 (2014) 447–501.
- [19] R.A. Smits, M. Adami, E.P. Istyastono, O.P. Zuiderveld, C.M. van Dam, F.J. de Kanter, A. Jongejan, G. Coruzzi, R. Leurs, I.J. de Esch, Synthesis and QSAR of quinazoline sulfonamides as highly potent human histamine H4 receptor inverse agonists, *J. Med. Chem.* 53 (2010) 2390–2400.
- [20] J.F.M. da Silva, M. Walters, S. Al-Damluji, C.R. Ganellin, Molecular features of the prazosin molecule required for activation of Transport-P, *Bioorg. Med. Chem.* 16 (2008) 7254–7263.
- [21] C. Xu, F.-C. Jia, Z.-W. Zhou, S.-J. Zheng, H. Li, A.-X. Wu, Copper-catalyzed multicomponent domino reaction of 2-bromoaldehydes, benzylamines, and sodium azide for the assembly of quinazoline derivatives, *J. Org. Chem.* 81 (2016) 3000–3006.
- [22] X. Wang, N. Jiao, Rh-and Cu-cocatalyzed aerobic oxidative approach to quinazolines via [4+ 2] C–H annulation with alkyl azides, *Org. Lett.* 18 (2016) 2150–2153.
- [23] X.Y. Mao, X.T. Lin, M. Yang, G.S. Chen, Y.L. Liu, Organocatalytic synthesis of gem-difluorinated C2-spiro indolines and pyrimido [1, 2-a] benzimidazoles from 2-Alkynyl-3, 3-Difluoro-3H-Indoles, *Adv. Synth. Catal.* 360 (2018) 3643–3648.
- [24] S. Lee, S.-O. Kim, H. Shin, H.-J. Yun, K. Yang, S.-K. Kwon, J.-J. Kim, Y.-H. Kim, Deep-blue phosphorescence from perfluoro carbonyl-substituted iridium complexes, *J. Am. Chem. Soc.* 135 (2013) 14321–14328.
- [25] X. Yang, Z. Wang, S. Madakuni, J. Li, G.E. Jabour, Efficient blue-and white-emitting electrophosphorescent devices based on platinum (II)[1, 3-Difluoro-4, 6-di (2-pyridinyl) benzene] Chloride, *Adv. Mater.* 20 (2008) 2405–2409.
- [26] W. Li, S. Albrecht, L. Yang, S. Roland, J.R. Tumbleston, T. McAfee, L. Yan, M.A. Kelly, H. Ade, D. Neher, Mobility-controlled performance of thick solar cells based on fluorinated copolymers, *J. Am. Chem. Soc.* 136 (2014) 15566–15576.
- [27] T. Lei, J.-H. Dou, Z.-J. Ma, C.-H. Yao, C.-J. Liu, J.-Y. Wang, J. Pei, Bipolar polymer field-effect transistors based on fluorinated isoindigo: high performance and improved ambient stability, *J. Am. Chem. Soc.* 134 (2012) 20025–20028.
- [28] D. O'Hagan, Understanding organofluorine chemistry. An introduction to the C–F bond, *Chem. Soc. Rev.* 37 (2008) 308–319.
- [29] S. Purser, P.R. Moore, S. Swallow, V. Gouverneur, Fluorine in medicinal chemistry, *Chem. Soc. Rev.* 37 (2008) 320–330.
- [30] Bruker, APEXII. Bruker AXS, Madison, WI, in, 2009.
- [31] M. COSMO. Bruker AXS, WI, COSMO. Bruker AXS, Madison, WI, in, 2009.
- [32] B.A. SAINT, Madison, WI, USA SAINT, Bruker AXS, Madison, WI, USA, in, 2009.
- [33] M. SADABS. Bruker AXS, WI, SADABS. Bruker AXS, Madison, WI, in, 2009.
- [34] G.M. Sheldrick, A short history of SHELX, *Acta Crystallogr., Sect. A: Found. Crystallogr.* 64 (2008) 112–122.
- [35] I. Macrae, J. Bruno, P. Chisholm, P. Edgington, E. McCabe, L. Pidcock, R. Rodriguez-Monge, J. Taylor, van de Streek, Wood, *J. Appl. Crystallogr.* 41 (2008) 466–470.
- [36] O.V. Dolomanov, L.J. Bourhis, R.J. Gildea, J.A. Howard, H. Puschmann, OLEX2: a complete structure solution, refinement and analysis program, *J. Appl. Crystallogr.* 42 (2009) 339–341.
- [37] G.M. Sheldrick, Crystal structure refinement with SHELXL, *Acta Crystallogr. C* 71 (2015) 3–8.
- [38] M. Turner, J. McKinnon, S. Wolff, D. Grimwood, P. Spackman, D. Jayatilaka, M. Spackman, CrystalExplorer17, University of Western Australia Crawley, Western Australia, Australia, 2017.
- [39] F.L. Hirshfeld, Bonded-atom fragments for describing molecular charge densities, *Theor. Chim. Acta* 44 (1977) 129–138.
- [40] M.A. Spackman, D. Jayatilaka, Hirshfeld surface analysis, *Cryst.Eng.Comm.* 11 (2009) 19–32.
- [41] M.A. Spackman, J.J. McKinnon, Fingerprinting intermolecular interactions in molecular crystals, *CrystEngComm* 4 (2002) 378–392.
- [42] F.H. Allen, O. Kennard, D.G. Watson, L. Brammer, A.G. Orpen, R. Taylor, Tables of bond lengths determined by X-ray and neutron diffraction. Part 1. Bond lengths in organic compounds, *J. Chem. Soc., Perkin Trans. 2* (1987) S1–S19.
- [43] S.K. Seth, N.C. Saha, S. Ghosh, T. Kar, Structural elucidation and electronic properties of two pyrazole derivatives: a combined X-ray, Hirshfeld surface analyses and quantum mechanical study, *Chem. Phys. Lett.* 506 (2011) 309–314.
- [44] M. Frisch, G. Trucks, H. Schlegel, G. Scuseria, M. Robb, J. Cheeseman, G. Scalmani, V. Barone, B. Mennucci, G. Petersson, Gaussian 09, Gaussian, Inc, Wallingford, CT, 2009.
- [45] C. Lee, W. Yang, R.G. Parr, Development of the Colle-Salvetti correlation-energy formula into a functional of the electron density, *Phys. Rev. B* 37 (1988) 785–789.
- [46] M. Tobe, Y. Isobe, H. Tomizawa, T. Nagasaki, H. Takahashi, T. Fukazawa, H. Hayashi, Discovery of quinazolines as a novel structural class of potent inhibitors of NF- κ B activation, *Bioorg. Med. Chem.* 11 (2003) 383–391.
- [47] J.-M. Noy, Y. Li, W. Smolan, P.J. Roth, Azide-para-Fluoro substitution on polymers: multipurpose Precursors for Efficient Sequential Postpolymerization Modification, *Macromolecules* 52 (2019) 3083–3091.
- [48] R.S. Kuryazov, N. Mukhamedov, D. Dushamov, R.Y. Okmanov, K.M. Shakhidoyatov, B. Tashkhodzayev, Quinazolines. 3^o. synthesis of 6-bro-

- mo-8-chloro-sulfonylquinazoline-2, 4 (1h, 3h)-dione and its interaction with nucleophilic reagents, *Chem. Heterocycl. Com+* 46 (2010) 585–591.
- [49] M. Sural, P. Funk, L. Kvapil, P. Hradil, J. Hlavác, V. Bertolasi, Study of anthranilate cyclisation to 2-hydroxymethyl-2, 3-dihydroquinazolin-4 (1H)-ones and an alternative synthetic route, *Arkivoc* 10 (2010) 255–265.
- [50] J.-i. Aihara, Correlation found between the HOMO–LUMO energy separation and the chemical reactivity at the most reactive site for isolated-pentagon isomers of fullerenes, *Phys. Chem. Chem. Phys* 2 (2000) 3121–3125.
- [51] A.D. Laurent, D. Jacquemin, TD-DFT benchmarks: a review, *Int. J. Quantum Chem* 113 (2013) 2019–2039.